



Missouri University of Science and Technology
Scholars' Mine

Physics Faculty Research & Creative Works

Physics

01 Jan 2005

Half-Metallicity and Efficient Spin Injection in AlN/GaN:Cr (0001) Heterostructure

Julia E. Medvedeva

Missouri University of Science and Technology, juliaem@mst.edu

X. Y. Cui

C. Stampfl

N. Newman

et. al. For a complete list of authors, see https://scholarsmine.mst.edu/phys_facwork/353

Follow this and additional works at: https://scholarsmine.mst.edu/phys_facwork

 Part of the [Physics Commons](#)

Recommended Citation

J. E. Medvedeva et al., "Half-Metallicity and Efficient Spin Injection in AlN/GaN:Cr (0001) Heterostructure," *Physical Review Letters*, American Physical Society (APS), Jan 2005.

The definitive version is available at <https://doi.org/10.1103/PhysRevLett.94.146602>

This Article - Journal is brought to you for free and open access by Scholars' Mine. It has been accepted for inclusion in Physics Faculty Research & Creative Works by an authorized administrator of Scholars' Mine. This work is protected by U. S. Copyright Law. Unauthorized use including reproduction for redistribution requires the permission of the copyright holder. For more information, please contact scholarsmine@mst.edu.

Half-Metallicity and Efficient Spin Injection in AlN/GaN:Cr (0001) Heterostructure

J. E. Medvedeva,¹ A. J. Freeman,¹ X. Y. Cui,² C. Stampfl,² and N. Newman³

¹*Physics and Astronomy Department, Northwestern University, Evanston, Illinois 60208-3112, USA*

²*School of Physics, University of Sydney, Sydney, Australia*

³*Chemical and Materials Engineering Department, Arizona State University, Tempe, Arizona 85287-6006, USA*

(Received 18 October 2004; published 15 April 2005)

First-principles investigations of the structural, electronic, and magnetic properties of Cr-doped AlN/GaN (0001) heterostructures reveal the possibility of efficient spin injection from a ferromagnetic GaN:Cr electrode through an AlN tunnel barrier. We demonstrate that Cr atoms segregate into the GaN region and that these interfaces retain their half-metallic behavior leading to a complete, i.e., 100%, spin polarization of the conduction electrons. This property makes the wide band-gap nitrides doped with Cr to be excellent candidates for high-efficiency magnetoelectronic devices.

DOI: 10.1103/PhysRevLett.94.146602

PACS numbers: 72.25.Hg, 71.20.-b, 75.70.Cn, 85.75.-d

The injection and manipulation of spin polarized carriers—a key feature determining successful spintronics—is highly dependent on phenomena and processes occurring at the interface between a ferromagnet and a semiconductor. It has been shown [1–3] that surface or interface sensitive approaches must be employed in both theory and experiment for the accurate determination of the spin polarization in materials proposed for potential magnetoelectronic devices. As perhaps the most striking example, Heusler compounds (such as NiMnSb, Co₂MnGe, Co₂CrAl)—which possess the appealing half-metallic ferromagnetic behavior in bulk—show significantly reduced spin polarization at the surface [1,2] or, consequently, at the interface with a semiconductor [3]. Indeed, first-principles calculations have revealed that the interface geometry essentially alters the electronic states and destroys half-metallicity [3].

Recently, nitride-based semiconductors, in particular, GaN and AlN, have attracted increasing attention for a number of reasons: (i) the introduction of magnetic dopants and achieving ferromagnetism in these materials provide complementary functionality to the wide range of devices already developed for pure large band-gap nitrides [4]. (ii) The shorter bond length and smaller spin-orbit coupling in these light-element compounds as compared to other III-V semiconductors (e.g., GaAs) are predicted to give rise to higher Curie temperatures [5]; indeed, recent measurements in Cr-doped GaN and AlN bulk showed T_c to be over 900 K [6]. (iii) The smaller spin-orbit interaction is also one of the main arguments for longer (by 3 orders of magnitude) electron spin lifetimes in GaN than in GaAs [7]. (iv) The III-N semiconductors appear to be much more resilient to the presence of extended structural defects than are other semiconductors [8]. While Cr-doped bulk GaN and AlN systems have been extensively studied [6,9–11], both experimental investigations and theoretical modeling of magnetically doped III-N interfaces—essential for practical spintronic applications—are lacking.

In this Letter, we present results of first-principles calculations of Cr-doped AlN/GaN (0001) heterostructures focusing on their structural, electronic, and magnetic properties. From a comparison of the formation energy of the relaxed AlN/GaN (graded Al_{1-x}Ga_xN/GaN) heterostructures with different site locations of Cr, we predict that the magnetic impurity segregates into the GaN region which serves as a ferromagnet, while AlN is the semiconductor part of the interface. Most significantly, we find that these interfaces retain the desired half-metallic behavior with a band gap in the spin minority channel of 2.7 eV, so that the conduction electrons can tunnel into the semiconductor material with 100% spin polarization. These findings make the wide band-gap nitride interfaces doped with Cr excellent candidates for applications based on spin transport.

The AlN/GaN (0001) interface is modeled using (1 × 1), (2 × 2), and (2 × 4) supercells of pure or Cr-doped wurtzite GaN and AlN (0001) with 3 double layers of each material; cf. Fig. 1. Note that a “double layer” is a single nitride layer; i.e., it consists of a group III element and nitrogen, so the (1 × 1), (2 × 2), and (2 × 4) super-

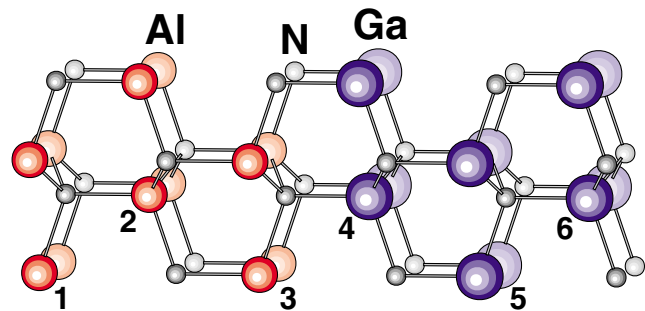


FIG. 1 (color online). Geometry of (2 × 2) AlN/GaN (0001) heterostructure: the large, intermediate, and small spheres correspond to Ga, Al, and N atoms, respectively. Substitutional site locations of Cr atoms in the supercell are denoted by numbers.

cells contain 12, 48, and 96 atoms, respectively. For the $\text{Al}_{1-x}\text{Ga}_x\text{N}/\text{GaN}$ (0001) heterostructures, we used (2×2) supercells with $x = 0.00, 0.25, 0.50, 0.75,$ and 1.00 in the layers; i.e., the content of Al (Ga) gradually decreases (increases) along the (0001) direction until a composition of pure GaN is formed. The equilibrium relaxed geometry of the structures was determined via total energy and atomic forces minimization for the lattice parameters a and c and the internal parameter u . Both the GaN and AlN regions of the heterostructure were allowed to relax with the same in-plane lattice constant [12], while the internal atomic relaxation for each lattice parameter c provided different minimized III-N distances along the (0001) direction. Note that during the optimization, *all* atoms were allowed to move in the $x, y,$ and z directions.

We employ the all-electron full-potential linearized augmented plane wave (FLAPW) method [13] that has no shape approximation for the potential and charge density. Cutoffs of the plane-wave basis (16.0 Ry) and potential representation (81.0 Ry), and expansion in terms of spherical harmonics with $\ell \leq 8$ inside the muffin-tin spheres, were used. Summations over the Brillouin zone were carried out using 32 special k points in the irreducible wedge. In addition to the local density approximation (LDA) for the ground-state properties, we used the self-consistent screened-exchange LDA (sX-LDA) method [14,15], which is known to provide a considerably improved description of the excited state (optical) properties as compared to the LDA or generalized gradient approximation (GGA) calculations.

We first determine the effect of the interface on the structural and electronic properties of pure AlN/GaN (0001) and compare with those of bulk GaN and AlN. Because of the lattice mismatch, both GaN and AlN are found to be mutually strained in the junction; cf. Table I: (i) the resulting in-plane lattice constant, 3.127 \AA , is 0.5% smaller (1.3% larger) than that of the bulk GaN (AlN) and is in agreement with the value observed [12] for the thinnest AlN/GaN bilayer, 3.134 \AA . (ii) The renormalized c lattice constant of GaN in the heterostructure is larger than that of AlN by 0.195 \AA which is approximately equal to the difference between the c parameters of the bulk materials; cf. Table I. We also found that away from the junctions, the Ga-N and Al-N distances along (0001) in each subunit tend

TABLE I. Calculated lattice parameters (\AA) and band-gap values (eV) for bulk wurtzite AlN and GaN and for the AlN/GaN (0001) heterostructure. Experimental data are taken from Ref. [16].

	Lattice parameters				Band gap		
	a	c	a_{exp}	c_{exp}	LDA	sX-LDA	Exp.
AlN	3.085	4.993	3.112	4.982	4.34	6.05	6.20
GaN	3.142	5.194	3.189	5.185	2.00	3.35	3.39
AlN/GaN	3.127	15.402			2.59	3.98	

to relax back towards those for GaN (AlN), which were calculated with fixed $a = 3.127 \text{ \AA}$ (cf. Table I) and optimized c parameters, and differ by 0.7% (0.9%) from these “bulk” values. Further, the structural relaxation at the junctions affects the electronic properties, in particular, the optical band gap of AlN/GaN (0001). In Table I, we present the band-gap values of bulk GaN and AlN and the (1×1) AlN/GaN (0001) calculated using both the LDA and sX-LDA methods. As expected, the LDA underestimates the band gap of both bulk GaN and AlN by 30%–40%, while the sX-LDA gives a considerably improved description—namely, a less than 2% difference from the experimental values. For the AlN/GaN (0001), we found that the valence band maximum and the conduction band minimum are formed by states of the GaN layers; thus, these states determine the calculated minimum band gap of the system to be 2.59 eV (3.98 eV) within the LDA (sX-LDA). In contrast, the states of the AlN layer located further away from the junctions lie deeper in the valence and conduction bands giving a band-gap increase of $\sim 0.4 \text{ eV}$ within both the LDA and sX-LDA.

Next, we investigated the effect of the interface on the transition-metal impurity location and the magnetic properties of the doped structure. To this end, we performed calculations of Cr doped substitutionally into the (2×2) AlN/GaN (0001). (For comparison of the electronic and magnetic properties, we also calculated Cr-doped bulk GaN and AlN.) The choice of the (2×2) supercell is motivated by the recently calculated critical separation between two Cr atoms in bulk GaN, $\sim 2.7 \text{ \AA}$, above which ferromagnetic (FM) coupling dominates the antiferromagnetic (AFM) one [11]. In our supercell case, the Cr-Cr distance is 6.3 \AA . Now, to find the preferred site location of the magnetic impurity, we calculated the formation energies [17] of six relaxed structures with cation-substituted Cr; cf. Fig. 1. The results, gathered in Table II, allow the following conclusions:

(i) The magnetic impurity segregates into the GaN region of the heterostructure which serves as a ferromagnet (as shown below), while the AlN region is a nonmagnetic part of the interface. The difference of the formation en-

TABLE II. Comparison of the calculated formation energies (eV) and the magnetic moments (μ_B) on the Cr atoms and its tetrahedral N neighbors in plane (N_{planar}) and along the (0001) direction (N_{apical}) for the Cr-doped (2×2) AlN/GaN (0001) with different Cr site locations (in parentheses) which correspond to those in Fig. 1.

	AlN region			GaN region		
	Cr(1)	Cr(2)	Cr(3)	Cr(4)	Cr(5)	Cr(6)
ΔE_f	+1.825	+1.817	+1.827	0.000	+0.031	+0.010
Cr	2.309	2.309	2.308	2.302	2.304	2.299
N_{planar}	-0.010	-0.011	-0.015	-0.020	-0.019	-0.016
N_{apical}	-0.018	-0.007	-0.005	-0.003	-0.012	-0.012

ergies for Cr in the AlN and in the GaN region of the heterostructure (~ 1.8 eV; cf. Table II) shows little dependence on the distance from the junctions [18] and agrees well with that for Cr-doped bulk GaN and AlN (2.0 eV).

(ii) The magnetic properties of the system are not strongly affected by the presence of the junctions: the calculated local magnetic moments on the Cr atoms in the AlN/GaN, Table II, are similar to those obtained for the corresponding relaxed Cr-doped bulk GaN ($2.304\mu_B$) and AlN ($2.313\mu_B$). We also found that the induced magnetic moments are larger on the N atoms which bond with Ga than on those connected to Al atoms by $0.006\mu_B$ (or $0.009\mu_B$) for planar (or apical) N atoms, on average [19]. Therefore, at the junction where the in-plane N atoms bond with Ga and the apical N atom bonds with Al, the induced in-plane spin polarization is dominant (case 4, Table II). In contrast, a higher spin polarization along (0001)—as compared to the in-plane magnetic moments—is observed at the other junction (case 1, Table II). Accordingly, we found the magnetic moments on planar and apical N atoms to be similar when Cr is equidistant from the junctions.

A contour plot of the calculated spin density distribution (case 4 in Table II) is presented in Fig. 2. In agreement with the itinerant $sp-d$ exchange model [20], the p orbital of the N atoms which points toward the Cr atom has its magnetic moment ($-0.048\mu_B$) antiparallel to the one on the magnetic impurity giving rise to FM coupling between two Cr atoms. (Note that the other two N p orbitals possess positive spin polarization resulting in a smaller magnetic moment, $-0.020\mu_B$, within the muffin-tin sphere; cf. Table II.) Indeed, from the (2×4) Cr-doped AlN/GaN (0001) supercell calculations, we confirm strong FM coupling between two Cr atoms with an energy difference between FM and AFM orderings of 97, 106, and 110 meV/Cr atom for case 4, 5, and 6, respectively. Accordingly, the effective exchange interaction parameters—estimated [21] to be 22, 26, and 28 meV, respectively—show a similar dependence on the Cr site

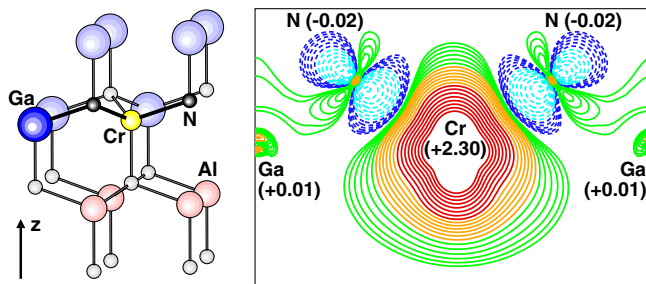


FIG. 2 (color online). Geometry of the most energetically favorable Cr site location in the AlN/GaN (0001) heterostructure (left) and contour plot of the calculated spin density distribution within a slice passing through this Cr atom and its planar N neighbors (right). Solid (dashed) lines in the plot denote positive (negative) spin polarization. The magnetic moments within the muffin-tin spheres, μ_B , are given in parentheses.

locations, which correlates with the decrease of the ratio between the induced magnetic moments on planar and apical N atoms; cf. Table II.

(iii) Regardless of the Cr site location in the GaN region of the interface (cf. cases 4–6 in Table II with a total energy difference of $\sim kT$), the three Cr-doped AlN/GaN systems share similar band structure features (the corresponding band offsets are discussed in a separate paper [22]): the magnetic impurity d states hybridized with the p states of the neighboring N atoms form deep bands in the nitride band gap; cf. Fig. 3. For the majority-spin channel, partially occupied triply degenerate t_{2g} and fully occupied doubly degenerate e_g bands are located at ~ 2.5 eV and ~ 1.1 eV, respectively, above the valence band maximum. The exchange interaction splits the Cr d states by ~ 2 eV. These findings are in agreement with previous studies [9,11] of Cr-doped bulk GaN.

Most significantly, we found that the Cr-doped AlN/GaN (0001) heterostructures retain the desired half-metallic behavior (consistent with the calculated integer total magnetic moment of $3\mu_B/\text{cell}$) with a band gap in the spin minority channel of ~ 2.7 eV; cf. Fig. 3. This leads to a complete, i.e., 100%, spin polarization of the conduction electrons and thus makes the system highly attractive for magnetoelectronic devices—specifically, magnetoresistive tunnel junctions.

Based on these results, in particular, on the preference of Cr atoms to substitute Ga rather than Al atoms in the AlN/GaN (0001), we model a realistic (in the sense of practical applications) magnetoelectronic system using (2×2) supercells of Cr-doped graded $\text{Al}_{1-x}\text{Ga}_x\text{N}/\text{GaN}$ (0001) heterostructures. From a comparison of the total energies for the relaxed structures with different Cr site locations (all of which are found to be half-metallic), we found that the magnetic impurity prefers to substitute the Ga atoms which are located in the pure GaN (0001) layers (cf. cases 7–14 in Fig. 4). A significant total energy increase is obtained for the structures where Cr substitutes

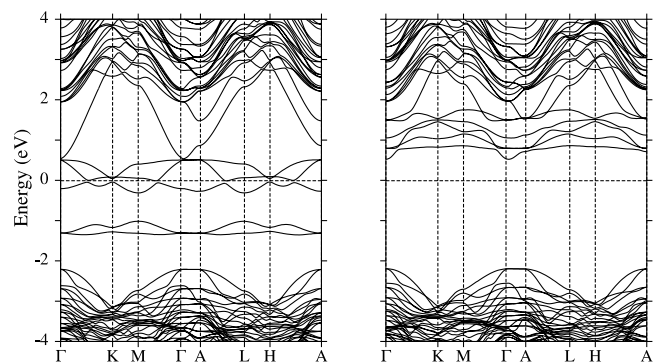


FIG. 3. Spin-resolved band structure along the high symmetry directions in the Brillouin zone for the most energetically favorable Cr-doped AlN/GaN (0001) heterostructure. The origin of the energy is taken at the Fermi level.

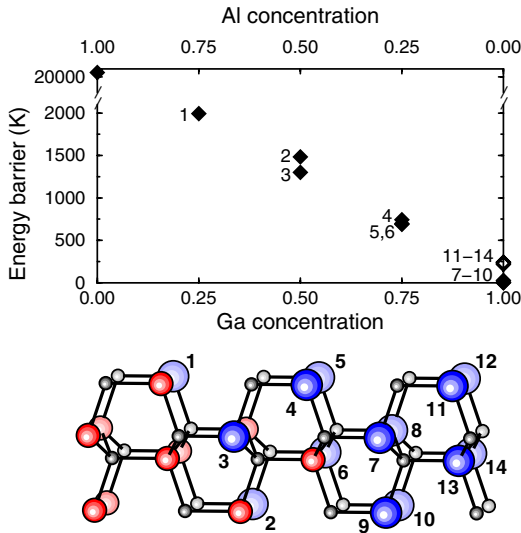


FIG. 4 (color online). Calculated relative formation energies, K, as a function of the cation concentration x in the Cr-doped graded $\text{Al}_{1-x}\text{Ga}_x\text{N}/\text{GaN}$ (0001) heterostructures and geometry of the corresponding supercell. The numbers on the graph correspond to those in the supercell and denote the Ga site locations substituted with a Cr atom.

the Ga atoms in the mixed nitride (0001) layers (cf. cases 1–6 in Fig. 4). This energy dependence on the composition suggests the possibility to control the width and height of the energy barrier by adjusting the Ga/Al ratio in the layers perpendicular to the growth direction—an important ingredient for device design optimization.

In summary, based on the first-principles calculations, we predict that efficient spin injection can be achieved using a ferromagnetic GaN:Cr electrode in conjunction with an AlN tunnel barrier. Since the Cr-doped AlN/GaN (0001) heterostructures are found to be half-metallic, we propose these wide band-gap nitride interfaces as candidates for high-efficiency magnetoelectronic devices which should exhibit a pronounced increase of magnetoresistance.

Work supported by DARPA (Grant No. 02-092-1/N00014-02-1-05918). Computational resources provided by the NSF supported National Center for Supercomputing Applications, Urbana-Champaign.

- [1] R.J. Soulen, Jr. *et al.*, *Science* **282**, 85 (1998); C.T. Tanaka, J. Nowak, and J.S. Moodera, *J. Appl. Phys.* **86**, 6239 (1999).
- [2] D. Ristoiu *et al.*, *Europhys. Lett.* **49**, 624 (2000).
- [3] G.A. de Wijs and R.A. de Groot, *Phys. Rev. B* **64**, 020402(R) (2001); S. Picozzi, A. Continenza, and A.J. Freeman, *J. Appl. Phys.* **94**, 4723 (2003); A. Debernardi, M. Peressi, and A. Baldereschi, *Mater. Sci. Eng., C* **23**, 743 (2003); I. Galanakis, cond-mat/0408204.

- [4] *Nitride Semiconductors: Handbook on Materials and Devices*, edited by P. Ruterana, M. Albrecht, and J. Neugebauer (Weinheim, Great Britain, 2003).
- [5] T. Dietl *et al.*, *Science* **287**, 1019 (2000).
- [6] H.X. Liu *et al.*, *Appl. Phys. Lett.* **85**, 4076 (2004); S.Y. Wu *et al.*, *Mater. Res. Soc. Symp. Proc.* **798**, Y10.57 (2004); D. Kumar, J. Antifakos, M.G. Blamire, and Z.H. Barber, *Appl. Phys. Lett.* **84**, 5004 (2004).
- [7] S. Krishnamurthy, M. van Schilfgaarde, and N. Newman, *Appl. Phys. Lett.* **83**, 1761 (2003).
- [8] S.D. Lester *et al.*, *Appl. Phys. Lett.* **66**, 1249 (1995).
- [9] M. van Schilfgaarde and O.N. Mryasov, *Phys. Rev. B* **63**, 233205 (2001).
- [10] S.E. Park *et al.*, *Appl. Phys. Lett.* **80**, 4187 (2002); S.G. Yang, A.B. Pakhomov, S.T. Hung, and C.Y. Wong, *Appl. Phys. Lett.* **81**, 2418 (2002); S.Y. Wu *et al.*, *Appl. Phys. Lett.* **82**, 3047 (2003).
- [11] G.P. Das, B.K. Rao, and P. Jena, *Phys. Rev. B* **69**, 214422 (2004).
- [12] Below the critical thickness of ~ 50 Å for GaN layers grown on AlN (0001), both GaN and AlN have the same in-plane lattice constant; see C. Kim, I.K. Robinson, J. Myoung, K.-H. Shim, and K. Kim, *J. Appl. Phys.* **85**, 4040 (1999).
- [13] E. Wimmer, H. Krakauer, M. Weinert, and A.J. Freeman, *Phys. Rev. B* **24**, 864 (1981).
- [14] R. Asahi, W. Mannstadt, and A.J. Freeman, *Phys. Rev. B* **59**, 7486 (1999).
- [15] We used cutoff parameters of 12.96 Ry in the wave vectors and $\ell \leq 3$ inside the muffin-tin spheres.
- [16] S. Strite and H. Morkoc, *J. Vac. Sci. Technol. B* **10**, 1237 (1992), and references therein.
- [17] We assume metal-rich growth conditions; i.e., the atom removed from (added to) the AlN/GaN is incorporated into (comes from) the corresponding bulk reservoir; thus, the formation energy is calculated as $E_f = E_{\text{int}} \cdot \text{Cr} - E_{\text{int}} - E_{\text{Ga(Al)}} + E_{\text{Cr}}$, where $E_{\text{int}} \cdot \text{Cr}$, E_{int} , $E_{\text{Ga(Al)}}$, and E_{Cr} are the total energy of the Cr-doped interface, the corresponding undoped interface, bulk orthorhombic Ga (fcc Al), and bcc Cr, respectively.
- [18] From additional calculations of Cr-doped (2×2) AlN/GaN (0001) with 5 double layers of each material, we found a negligible variation in the formation energies (< 0.04 eV) across the heterostructure.
- [19] We also found that the Cr induced magnetic moments on its neighboring Ga atoms ($\sim 0.014\mu_B$) are larger than those on the Al atoms ($\sim 0.010\mu_B$). This finding can be explained by the fact that the states of the AlN layers lie deeper in the valence band and hence they are more screened as compared to the GaN layers.
- [20] J. Kanamori and K. Terakura, *J. Phys. Soc. Jpn.* **70**, 1433 (2001).
- [21] Within the linear muffin-tin orbital method in the atomic sphere approximation, the effective exchange interaction parameters were calculated as a second derivative of the ground-state energy with respect to the magnetic moment rotation angle; see A.I. Liechtenstein, M.I. Katsnelson, V.P. Antropov, and V.A. Gubanov, *J. Magn. Magn. Mater.* **67**, 65 (1987).
- [22] J.E. Medvedeva *et al.* (to be published).